Correspondence to:
A. Tangarife-Escobar,
atanga@bgc-jena.mpg.de

Radiocarbon Isotopic Disequilibrium Shows Little Incorporation of New Carbon in Mineral Soils of a Boreal Forest Ecosystem

Andrés Tangarife-Escobar[1] [ID], **Georg Guggenberger[2]** [ID], **Xiaojuan Feng[3]** [ID], **Estefanía Muñoz[1,4]**, **Ingrid Chanca[1,5,6]** [ID], **Matthias Peichl[7]**, **Paul Smith[8]** [ID], and **Carlos A. Sierra[1]** [ID]

[1]Department of Biogeochemical Processes, Max Planck Institute for Biogeochemistry, Jena, Germany, [2]Institute of Earth System Sciences, Section Soil Science, Leibniz Universität Hannover, Hannover, Germany, [3]State Key Laboratory of Vegetation and Environmental Change, Institute of Botany, Chinese Academy of Sciences, Beijing, China, [4]CREAF, Barcelona, Spain, [5]Laboratoire des Sciences du Climat et de l'Environnement, Gif-sur-Yvette, France, [6]Laboratório de Radiocarbono, Instituto de Física, Universidade Federal Fluminense, Niterói, Brazil, [7]Department of Forest Ecology and Management, Swedish University of Agricultural Sciences (SLU), Umeå, Sweden, [8]Unit for Field-Based Forest Research, Swedish University of Agricultural Sciences (SLU), Vindeln, Sweden

Abstract Boreal forests fix substantial amounts of atmospheric carbon (C). However, the timescales at which this C is cycled through the ecosystem are not yet well understood. To elucidate the temporal dynamics between photosynthesis, allocation and respiration, we assessed the radiocarbon (^{14}C) disequilibrium (*D*) between different C pools and the current atmosphere to understand the fate of C in a boreal forest ecosystem. Samples of vegetation, fungi, soil and atmospheric CO_2 were collected at the Integrated Carbon Observation System station Svartberget in northern Sweden. Additionally, we analyzed the Δ^{14}C-CO_2 from incubated topsoil and forest floor soil respiration (FFSR) collected over a 24-hr cycle, and calculated the Δ^{14}C signature of the total ecosystem respiration (*Re*) using the Miller-Tans method. We found that vegetation pools presented a positive *D* enriched with bomb ^{14}C, suggesting a fast-cycling rate (months to years) for living biomass and intermediate (years to decades) for dead biomass. In contrast, mineral soils showed a negative *D*, indicating minimal incorporation of bomb ^{14}C. FFSR showed diurnal Δ^{14}C variability (mean = 8.5‰), suggesting predominance of autotrophic respiration of recently fixed labile C. Calculations for Δ^{14}C in *Re* (median = 12.7‰) demonstrate the predominance of C fixed from days to decades. Although the boreal forest stores significant amounts of C, most of it is in the soil organic layer and the vegetation, where it is cycled relatively fast. Only minimal amounts of recent C are incorporated into the mineral soil over long timescales despite the current stocks in soils being relatively old.

Plain Language Summary Boreal forests play a key role as an alternative to sequester carbon dioxide (CO_2) from the atmosphere and mitigate climate change. However, there is uncertainty on where this CO_2 is stored and the timescales at which it remains. To understand this, we studied the fate of the atmospheric CO_2 since the beginning of the nuclear era (1950s) by measuring the radiocarbon content of vegetation, fungi, soil, forest floor soil respiration and atmospheric air from a boreal forest stand in northern Sweden. We found that vegetation stores carbon from months (in leaves and moss) to decades (in litter layer and wood debris), while the soil organic layer presented carbon even older than a century. In contrast, mineral soils contained little recent carbon along with low content of organic carbon. The analysis of FFSR revealed that carbon comes mainly from recently fixed carbon, while the overall ecosystem respiration reflected a mix of carbon sources, ranging from days to decades. Overall, the boreal forest stores substantial amounts of carbon, but most of it moves relatively fast through the ecosystem. Only a small amount of new carbon is added to the mineral soil where it remains for long timescales.

1. Introduction

An accurate assessment of carbon (C) storage and cycling rates in boreal forest ecosystems is crucial to better understand the effectiveness of climate change mitigation strategies (Lundmark et al., 2014; Peichl et al., 2023) and to project future climate scenarios. As measures to reduce atmospheric carbon dioxide (CO_2) concentrations become increasingly important, understanding ecosystem C storage in ecosystems with substantial reservoirs is essential, especially at timescales relevant for management and policy outcomes (Crow & Sierra, 2022; Lal
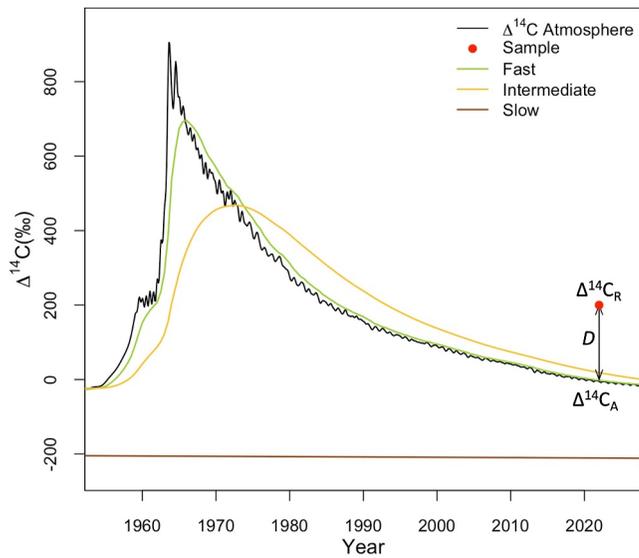
Figure 1. Schematic diagram of ^{14}C isotopic disequilibrium (*D*) for a fast (green line), intermediate (yellow line) and slow-cycling (brown) C system. The radiocarbon content in respired CO_2 or bulk material ($\Delta^{14}C_R$) represents the atmospheric Δ^{14}C value of the C at the time it was photosynthesized by plants. On the other hand, the current Δ^{14}C values of atmospheric CO_2 ($\Delta^{14}C_A$) corresponds with the CO_2 photosynthesized in the present. The red dot represents a sample taken from any specific year with a known atmospheric Δ^{14}C value, following the curve proposed by Hua et al. (2022). The $D = \Delta^{14}C_R - \Delta^{14}C_A$ can be $D > 0$ (positive *D*), $D < 0$ (negative *D*) or $D = 0$ (in equilibrium).

et al., 2021). The ability of a reservoir to capture and store CO_2 depends on both the magnitude of C fluxes and the duration of C storage (Matthews et al., 2023; Randerson et al., 2002; Trumbore et al., 1996). C reservoirs with low storage capacity and fast-cycling rates may not be suitable for prolonged C sequestration, whereas large reservoirs with slow-cycling rates can absorb and store C over decades, partially offsetting fossil fuels emissions (Trumbore, 2000).

Radiocarbon (^{14}C) measurements in soil and vegetation pools, both in CO_2 and in bulk material, provide useful insights into the average time that C has remained in ecosystems, from fixation from the atmosphere until its respiration by autotrophs or heterotrophs (Balesdent, 1987; Trumbore et al., 1996). This technique takes into account that (a) the decrease in ^{14}C (in an isolated sample) is due to radioactive decay, (b) the excess of bomb ^{14}C in the atmosphere following thermonuclear weapons testing in the early 1950s, and (c) the ongoing decrease in atmospheric ^{14}C levels due to its assimilation by oceanic and terrestrial reservoirs and the dilution by ^{14}C-free CO_2 from fossil fuel emissions (Keeling, 1979; Phillips et al., 2015; Suess, 1955). At the present time, atmospheric Δ^{14}C values have returned to pre-bomb levels, with Δ^{14}C already below zero, creating a unique opportunity to assess the fate of atmospheric C since the introduction of bomb ^{14}C. Given variable C storage periods in ecosystem biomass, the Δ^{14}C of bulk materials and respired CO_2 ($\Delta^{14}C_R$) is expected to differ from the current atmospheric Δ^{14}C of CO_2 ($\Delta^{14}C_A$), with the biosphere returning excess radiocarbon to the atmosphere resulting in the ^{14}C isotopic disequilibrium (*D*) (Figure 1) (Bowling et al., 2014; Eglinton et al., 2023; Fung et al., 1997; Gaudinski et al., 2000; Thompson & Randerson, 1999).

To assess relative *D* over time, the atmosphere serves as the logical reference since it accounts with a well-documented ^{14}C concentration for the last 14,000 calendar years that can be extended to 50,000 years (Reimer et al., 2013; Soulet et al., 2016). Until the 1990s, the decline in $^{14}CO_2$ was mainly due to the transfer of atmospheric ^{14}C bomb to the oceans and terrestrial biosphere, where soils and plants had lower ^{14}C content than the atmosphere (Naegler & Levin, 2009). However, the primary imbalance today is the release of ^{14}C-free fossil CO_2 (Levin et al., 2010). As the atmosphere becomes increasingly depleted of ^{14}C, the biosphere follows this depletion with a time lag (Tans et al., 1993). Calculations of *D* can provide information on the "age" of C in different reservoirs (LaFranchi et al., 2016) and therefore differentiate between fast and slow C cycling (Phillips et al., 2015; Thompson & Randerson, 1999; Xiong et al., 2017). We define fast cycling as occurring within 0–2 years, intermediate cycling between 2 and 60 years, and slow cycling as taking longer than 60 years (before the bomb peak). For example, soils gaining C in recent decades will contain bomb ^{14}C, yielding positive *D* and suggesting fast to intermediate cycling rates of C in soils, while soils without content of bomb ^{14}C will result in negative *D* due to radioactive decay (De Camargo et al., 1999; Trumbore et al., 1995). *D* variation patterns facilitates the assessment of ecosystems and soils subjected to different land management practices and the impact of climate change on C cycling in regions with substantial carbon stocks, such as the boreal region.

Boreal forests are an important component of the global C cycle (Bradshaw & Warkentin, 2015; Peichl et al., 2023; Price et al., 1999), containing one-third of the world's forests area and about 30% of C present in the terrestrial biome (Kasischke, 2000), generally acting as a net sink of CO_2 (Yang et al., 2023). However, there are current concerns that the boreal region is shifting toward a net source of CO_2 (Alster et al., 2020; Zhao et al., 2021). To better understand these changes in the sink/source status of the boreal forests, it is useful to analyze temporal changes in Δ^{14}C in different ecosystem pools and in respired C. Multiple studies have demonstrated differences in soil respiration ^{14}C content compared to atmospheric levels, influenced by the duration of organic matter in the soil and the contribution of root respiration to CO_2 production (Carbone et al., 2008; Czimczik et al., 2006; Dörr & Münnich, 1986). For example, freshly assimilated plant C is rapidly

transported and selectively used for belowground soil respiration, especially in late morning hours (Bahn et al., 2009). Conversely, photosynthates from previous days dominate respiration substrates during night and early morning hours (Bahn et al., 2009). Variation of C stocks and cycling times has been observed to be modulated by climatic, edaphic, biological, hydrological (Hopkins et al., 2014; McFarlane et al., 2013) and soil frost factors (Muhr et al., 2009). The use of D in ^{14}C offers critical understanding into temporal C cycle variations, especially in recent decades, and spatial distribution when analyzed across a diverse pool range.

In this study, we address two specific questions: (a) What is the variation in Δ^{14}C among different ecosystem pools in a boreal forest, and what insights can be gained about their D? and (b) How does the D of Δ^{14}C vary in different C pools and the respired fractions within a boreal forest ecosystem? We hypothesize that, given the role of the Northern Hemisphere as an important C sink, a strong ^{14}C incorporation in vegetation and superficial soil layers would be expected in boreal forest ecosystems, leading to positive D values. Alternatively, based on recent work on C transit times that show fast cycling of carbon for soils (Lu et al., 2018; Sierra et al., 2018, 2023; Xiao et al., 2022), we would expect that newly fixed C may not be incorporated in slow-cycling pools for extended periods, resulting in negative D values for the mineral soil.

This study integrates ^{14}C measurements from soil, vegetation and forest floor soil respiration (FFSR) to calculate D and constrain the incorporation of new C (^{14}C bomb) in different pools of the boreal forest ecosystem, revealing the temporal dynamics of its cycling. Additionally, we utilize Δ^{14}C calculations derived from atmospheric CO_2 at different heights below the canopy to understand the relative contribution of ecosystem pools to the signature of the total ecosystem respiration (Re). This analytical framework facilitates the interpretation of primary CO_2 sources and the implications on the C storage patterns within the boreal forest.

2. Data and Methods

2.1. Site Description

This study was conducted at a boreal forest site equipped with an atmospheric-ecosystem infrastructure composed by a 150-m tall tower from the Integrated Carbon Observation System (ICOS). It is located in the Experimental Forests of the Swedish University of Agricultural Sciences at the Svarberget (SVB) Research Station (64.2443 N; 19.7663 E; 230 m a.s.l.) in the Krycklan catchment, 60 km inland from Umeå, Northern Sweden (Figure 2). The sampling points were selected based on a random selection of coordinates around a circular area of 25 m radius with center at the ICOS tall tower, covering a total area of 1963 m^2 (Figure 2d). The land use in the catchment is dominated by forestry and approximately 25% has been protected since 1922 with the experimental forest around the SVB station being excluded from harvest. The forest stand adjacent to the sampling site is estimated to be approximately 111 years old (up to 2024) (Laudon et al., 2013). Vegetation cover consists mainly of *Pinus sylvestris*, followed by *Picea abies* and some *Betula spp* (Chi et al., 2020). Soils are predominantly iron podzols developed from till and sorted sediments (Chi et al., 2020; Erdbrügger et al., 2023). The climate is classified as cold-temperate and humid. Over a 40-year period, the average duration of winter snow cover is 167 days, but this has been declining since the 1980s (1981–2010) (Laudon et al., 2021). Mean annual temperature is 1.8°C and mean annual precipitation is 614 mm (Laudon et al., 2013, 2021).

2.2. Soil Respiration Sampling for Radiocarbon Analysis

We collected 24 samples of FFSR over a 24-hr cycle for a period of four days from 13/8/2022 to 16/8/2022 from four randomly selected spots within the forest stand around the ICOS tower. We define FFSR here as the CO_2 released from the soil along with herbaceous vegetation up to the height of our collection chambers at 10 cm. The sampling scheme comprised four PVC dark chambers inserted 5 cm into the soil 3 weeks before gas collection, expected to provide enough buffer time to avoid influence from biomass damage/disturbance (Kwon et al., 2016; Pavelka et al., 2018). Soil respiration was collected at 3 hr intervals (6:00, 9:00, 12:00, 15:00, 18:00 and 21:00), collecting the gas accumulated in the headspace of the chambers from the previous 3 hr, except for the samples taken at 6:00, which accumulated the flux from 21:00 of the previous day. Each of the sampling intervals was replicated in each of the four chambers to consider spatial variability (Betson et al., 2007).

The respiration chambers were attached to a self-manufactured mini-sampler, which included a water trap (magnesium perchlorate), a CO_2 sensor (ExplorIR, Gas Sensing Solutions, UK) and a pump (NPM015, KNF,
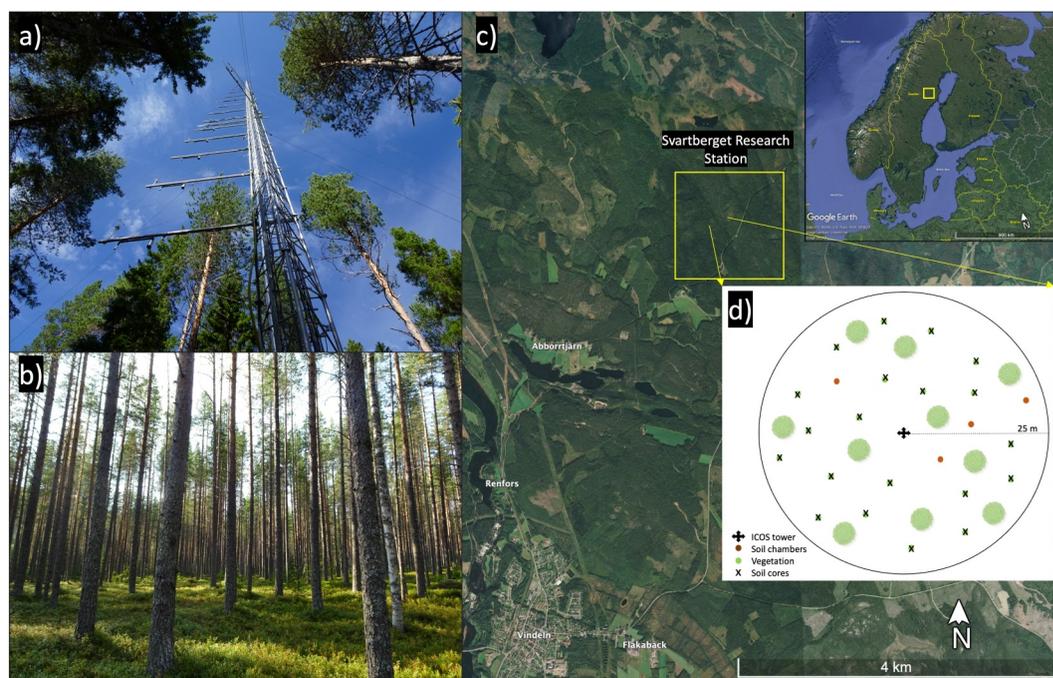
Figure 2. Regional and detailed overview of the study site. (a) The Integrated Carbon Observation System tower in the center of the sampling arrangement, (b) view of the sampled forest stand, (c) location of the Svarberget Research Station, and (d) schematic distribution of the randomly selected sampling points: 20 for soil cores and vegetation and four for soil chambers. Regional map data: Google, © 2023 CNES/Airbus, © 2023 Landmäteriet/Metria. Continental map data: Google, Data SIO, NOAA, U.S. Navy, NGA, GEBCO. Image Landsat/Copernicus. Image IBCAO.

Germany). This mini-sampler was adapted after Garnett et al. (2021). Before the beginning of respiration accumulation, the gas inside the entire sampling system was scrubbed by pumping and circulation through a soda lime cartridge for 15 min, after that, the initial time for FFSR accumulation started. Then, the accumulated flux from the chambers was pumped through the water trap and stored in zeolite (Type 13X, 1.6 mm pellets, Sigma-Aldrich, UK) molecular sieve cartridges (Walker et al., 2015; Wotte et al., 2017) for subsequent ^{14}C analysis.

2.3. Soil, Fungi, and Vegetation Sampling

A total of 20 sampling points were selected using a random sampling approach within the area enclosed by a circle of 25 m radius around the ICOS tall tower. At each point, we recovered one soil core (20 in total) by using a soil auger to a depth of 30 cm. Consequently, we separated the cores every 5 cm to analyze changes in Δ^{14}C and C content through depth. Some sections of the cores were not retrieved and therefore the amount of analyzed samples varied over depth (see "Samples" column in Table 1). At the study site, the topsoil layer (0–5 cm) generally corresponds to the organic layer, while the lower layer (5–30 cm) represents the mineral soil. From these soil cores, stones were extracted and fine roots (< 3 mm) were separated from the organic soil and the uppermost mineral soil layers, 0–5 and 5–10 cm, respectively. To ensure comprehensive sampling, 6 different compartments of vegetation material were collected around the soil core points. Foliage from trees and shrubs consisted of leaves and needles accessible by hand. Coarse woody debris (CWD) comprised fallen tree sections and branches found on the ground. Wood samples were obtained from the nearest tree by drilling cores up to 15 cm deep into live standing trees using a 0.7 mm auger. Moss and litter layers were systematically collected around the soil core points, maintaining spatial heterogeneity within a three-m radius. Fruiting bodies of mycorrhizal fungi were sampled from the soil surface at 6 of the 20 sampling spots. In total, we obtained 99 samples for soil, 120 for vegetation, 40 for fine roots and 6 for fungi. The collected samples were air-dried at 40°C and ground for laboratory analyses. All soil samples were analyzed for total organic carbon (TOC), total inorganic carbon (TIC) and Δ^{14}C. As for the vegetation samples and fine roots, 5 and 10 samples were randomly chosen, respectively, for the above-mentioned analysis (except TIC) as well as for Δ^{14}C.

Table 1
$\Delta^{14}C$ Statistics for Each Pool in the Boreal Forest Stand

Pool	Samples	Mean	Median	σ	Min.	Max.	p-value
Atmosphere[a]	4	−2.3	−3.5	4.7	−6.6	4.3	
Re	52	42.8	12.7	75.9	−15.0	363.8	
FFSR	35	8.5	13.6	20.9	−55.4	25.3	0.024
Soil inc. 0–5	4	65.3	65.0	3.6	61.5	69.5	0.176
Soil inc. 5–10	2	58.3	58.3	0.8	57.7	58.8	0.025
Wood	20	140.7	128.3	58.9	42.0	254.4	< 0.01
Tree foliage	20	2.9	1.8	3.5	−3.6	8.7	< 0.01
Shrub foliage	20	1.2	1.4	4.7	−6.6	16.8	< 0.01
Moss	20	7.8	7.3	2.8	2.6	12.8	< 0.01
Litter layer	20	68.4	54.3	51.5	11.3	195.8	< 0.01
CWD	20	105.2	69.1	115.4	−25.0	329.9	< 0.01
Fungi	6	−2.7	−2.6	1.8	−5.9	−0.9	0.833
Soil 0–5	19	55.6	63.5	54.5	−96.6	136.1	< 0.01
Soil 5–10	20	−133.7	−100.6	139.2	−444.7	83.8	< 0.01
Soil 10–15	20	−188.2	−175.4	133.1	−432.5	39.2	< 0.01
Soil 15–20	18	−152.5	−116.1	131.2	−394.0	47.7	< 0.01
Soil 20–25	13	−153.5	−128.9	114.6	−466.5	−15.2	< 0.01
Soil 25–30	9	−204.9	−212.5	124.2	−461.9	−6.1	< 0.01
Roots 0–5	10	77.0	76.4	53.1	−7.5	186.2	< 0.01
Roots 5–10	10	98.4	92.0	90.0	−44.9	250.3	< 0.01

Note. The second column indicates the number of samples used for the calculations. σ shows the standard deviation, and Min. and Max. indicate the minimum and maximum values within the evaluated range of data for each pool. The p-values indicate the statistical significance of the difference between the $\Delta^{14}C$ values of each pool compared to the atmospheric background. [a]Atmospheric background.

2.4. Soil Incubation

Soil samples were incubated without roots. Two representative samples for the organic layer and topmost mineral soil (5–10 cm depth) were produced by mixing 10 samples from the original 20 sampling spots. Four analytical replicates from each of these 2 samples were incubated following the methodology reported in Tangarife-Escobar, Guggenberger, Feng, Dai, et al. (2024) with the aim to obtain the $\Delta^{14}C$-CO_2 signature of the incubated soils. Specifically, 22 g (0–5 cm) and 97 g (5–10 cm) of dry soil were incubated in 587 mL flasks under room temperature after adding 30% of their total mass in water. CO_2 concentrations were measured at intervals of 5 days using a CO_2 analyzer LI-COR 6262. Incubations were ended simultaneously on the seventeenth day until respiration fluxes stopped increasing and every sample had a minimal estimated concentration of CO_2-C in the headspace equivalent to 2 mg of C, enough for radiocarbon analyses. Concentrations between 6,800 and 7,400 ppm of CO_2 were reached in the flasks after the incubation time.

2.5. Atmospheric CO_2 Measurements and the ICOS Data Set

The collection of air samples for isotopic analyses was based on the historical record of CO_2 concentration measurements at the ICOS-SVB station (Drought 2018 Team and ICOS Atmosphere Thematic Centre, 2020; ICOS RI et al., 2022). This data set contains information from 15 heights, from 4.2 to 150 m with a temporal resolution of 30 min. The data spans seven years (2014–2020). Missing values were partially filled using a forecasting algorithm based on the exponential smoothing method (Muñoz & Sierra, 2023), reaching a percentage of missing values of around 27% for all heights. Figure 3a shows the diurnal cycle with a half-hour resolution for 8 of the 15 heights. Each point on the lines corresponds to the mean of the concentrations of the 31 days of August during the 7 years at half-hour resolution and the bars are the standard error of the mean. Figure 3b shows the
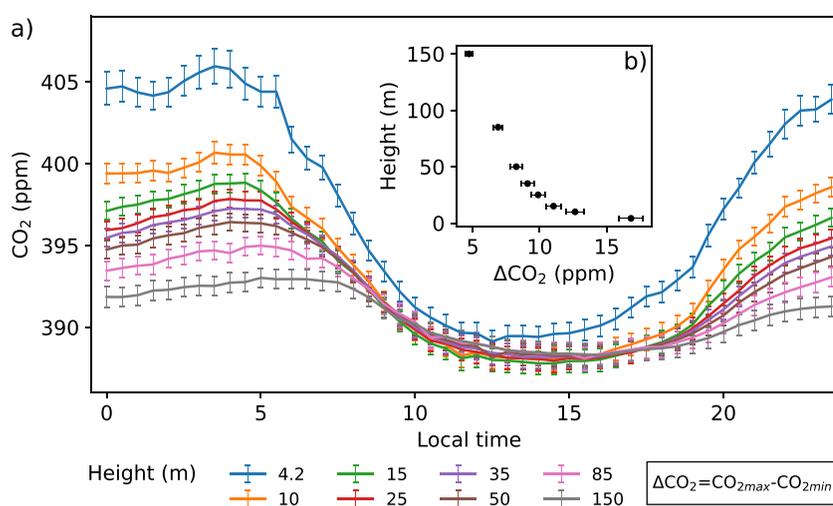
Figure 3. Half-hourly averaged CO_2 diurnal cycle (a) and difference between the maximum and the minimum averaged value throughout the day (ΔCO_2) (b) at different heights at the Integrated Carbon Observation System SVB site in August. Bars in panel (a) indicate the standard error of the mean.

maximum differences in the half-hour means ($\Delta CO_2 = \Delta CO_{2max} - \Delta CO_{2min}$) at 8 heights. Figures 3a and 3b indicate that, in general, CO_2 concentrations decrease as the height increases, as well as their variability during the day. Furthermore, the peak concentration occurs around 03:00 to 05:00 hr local time, and the lowest concentration between 12:00 and 16:00 hr.

As the calculation of the $\Delta^{14}C$ of total Re through the Miller-Tans methodology described below requires a large gradient between the CO_2 concentrations, we decided to carry out the field campaign in August, the month in which the maximum differences have historically been observed, reaching ΔCO_2 values of 16.8 μmol mol^{-1} at 4.2 m (see blue line in Figures 3a and 3b). The times for collecting air samples were defined according to the peaks and valleys of CO_2, and the maximum height of 150 m was selected as the background atmospheric ^{14}C level. The latter, is because the concentrations at this height have little influence on the dynamics occurring below the canopy. The average value of $\Delta^{14}C$ in atmospheric CO_2 for the month of August (2022) was calculated based on four measurements at 150-m height, which was taken as the reference value to define the D.

Air samples were collected in glass flaks of 2 or 3 L, with air compressed at 1.4 bar using a portable flask sampler (Heimann et al., 2022), and sampling at heights of 0.8, 4, 7, 10, 20, and 32.5 m. Samples were collected at regular intervals during day and night, from 12/08/2022 until 16/08/2022, to cover an entire diurnal cycle (Figure A1).

2.6. Radiocarbon Measurements

After preparation, the plant, soil, ambient air, and FFSR samples were processed at the radiocarbon laboratory of the Max Planck Institute for Biogeochemistry in Jena, Germany. The laboratory requires a minimal sample size of 0.5 mg C for both gas and solid samples (Steinhof et al., 2017). Molecular sieves with FFSR and flasks with atmospheric air were purified on a vacuum line to isolate the CO_2. Subsequently, pure CO_2 samples were reduced to graphite using H_2 with Fe as a catalyst for the graphitization reaction. $^{14}C/^{12}C$ ratios were determined by Accelerator Mass Spectrometry with a MICADAS (Mini Radiocarbon Dating System, IonPlus, Switzerland).

Radiocarbon data are reported as $\Delta^{14}C$ and adjusted to account for mass-dependent fractionation by normalizing to a $\delta^{13}C$ value of $-25‰$ divided by 0.95 times the measured ratio of the Oxalic Acid I standard (OX-I) (Stuiver & Polach, 1977). The values are expressed as a percentage of Modern Carbon, which can be converted to $F^{14}C$ by dividing by 100 and subsequently transformed to $\Delta^{14}C$ with the equation (Stuiver & Polach, 1977)

$$\Delta^{14}C = \left[F^{14}Ce^{\lambda_C(1950-t)} - 1\right] \times 1000[‰], \tag{1}$$

where $F^{14}C$ denotes the Fraction Modern. The parameter λ_C stands for the revised radiocarbon decay constant equivalent to $1/8267$ (y^{-1}), while t represents the year of sample measurement.

2.7. Data Analysis

Isotopic disequilibrium in the different ecosystem pools was calculated by subtracting the $\Delta^{14}C$ value of the atmospheric background $\left(\Delta^{14}C_A\right)$ from the $\Delta^{14}C$ of the respective pool as

$$D = \Delta^{14}C_R - \Delta^{14}C_A. \tag{2}$$

Statistical analyses were conducted using R version 4.3.2 to assess variations in $\Delta^{14}C$ within and between pools. ANOVA was employed to compare live and dead biomass, with post-hoc analysis performed using Tukey's HSD test. For soil incubation data, where sample sizes were unequal, we used Welch's t-test. An independent t-test was applied to evaluate roots, assuming equal variances, while a Wilcoxon test was used for FFSR due to nonnormal distribution of residuals. For bulk soil analysis, which involves non-normally distributed data and unequal sample sizes, the Kruskal-Wallis test was used.

For the calculation of the radiocarbon signature of total Re, we used a two-end-member mixing model to separate the isotopic signature of respiration from that of the background air. The approach is commonly known as the Miller-Tans method or canopy-minus-background method (Miller & Tans, 2003; Phillips et al., 2015), in which the isotopic signature of respired CO_2 is obtained by manipulating two mass balance equations and fitting a Type II linear regression to the data. The Miller-Tans method is a modification of the Keeling plot method (Keeling, 1958, 1961) used to determine the isotopic composition of the main source of ecosystem respiration, but allowing explicit specification of background values. Therefore, the Miller-Tans approach does not rely on the assumption of a constant background as the Keeling approach. Both methods assume that the CO_2 concentration below the canopy ($CO_{2_{obs}}$) is the mix of CO_2 from the background ($CO_{2_{bk}}$) atmospheric air and CO_2 released by respiration of soils and plants ($CO_{2_{Re}}$) in the ambient air; additionally, as the product of isotopic signature and CO_2 concentration is conserved (Tans, 1980), the isotopic mixing in CO_2 below the canopy is proportional to the concentration of CO_2 in the background and in the ecosystem respiration (Re). These assumptions, considering the Miller-Tans method and using the $F^{14}C$ notation, lead to:

$$\Delta\left(F^{14}C \cdot CO_2\right) = F^{14}C_{Re} \cdot \Delta CO_2 \tag{3}$$

where

$$\Delta CO_2 = CO_{2_{obs}} - CO_{2_{bk}} \tag{4}$$

$$\Delta\left(F^{14}C \cdot CO_2\right) = F^{14}C_{obs} \cdot CO_{2_{obs}} - F^{14}C_{bk} \cdot CO_{2_{bk}} \tag{5}$$

Thus, the slope of the regression between ΔCO_2 and $\Delta(F^{14}C \cdot CO_2)$ provides an estimate of the radiocarbon signature of (Re) (see Figure A2).

To obtain an estimate of uncertainty in the radiocarbon signature of Re, we performed a bootstrap analysis fitting the Type II regression with different combinations of data from the 6 sampling heights (ranging from 0.8 to 32.5 m) and keeping 150 m exclusively for the background. We repeated the analysis 50,000 times by randomly selecting the number of heights, obtaining 45,780 valid combinations. Regressions were performed only when there were more than 10 data points available. The results were transformed back to $\Delta^{14}C$ notation and interpreted based on their mean and median values.

3. Results

Carbon content analysis indicated a high concentration of TOC (percent organic carbon) predominantly in vegetation and fungi material (Table A1) with mean values exceeding 45%. TOC exhibited a decreasing trend with soil depth, as depicted in Figure A3, with elevated percentages observed exclusively in the organic layer and
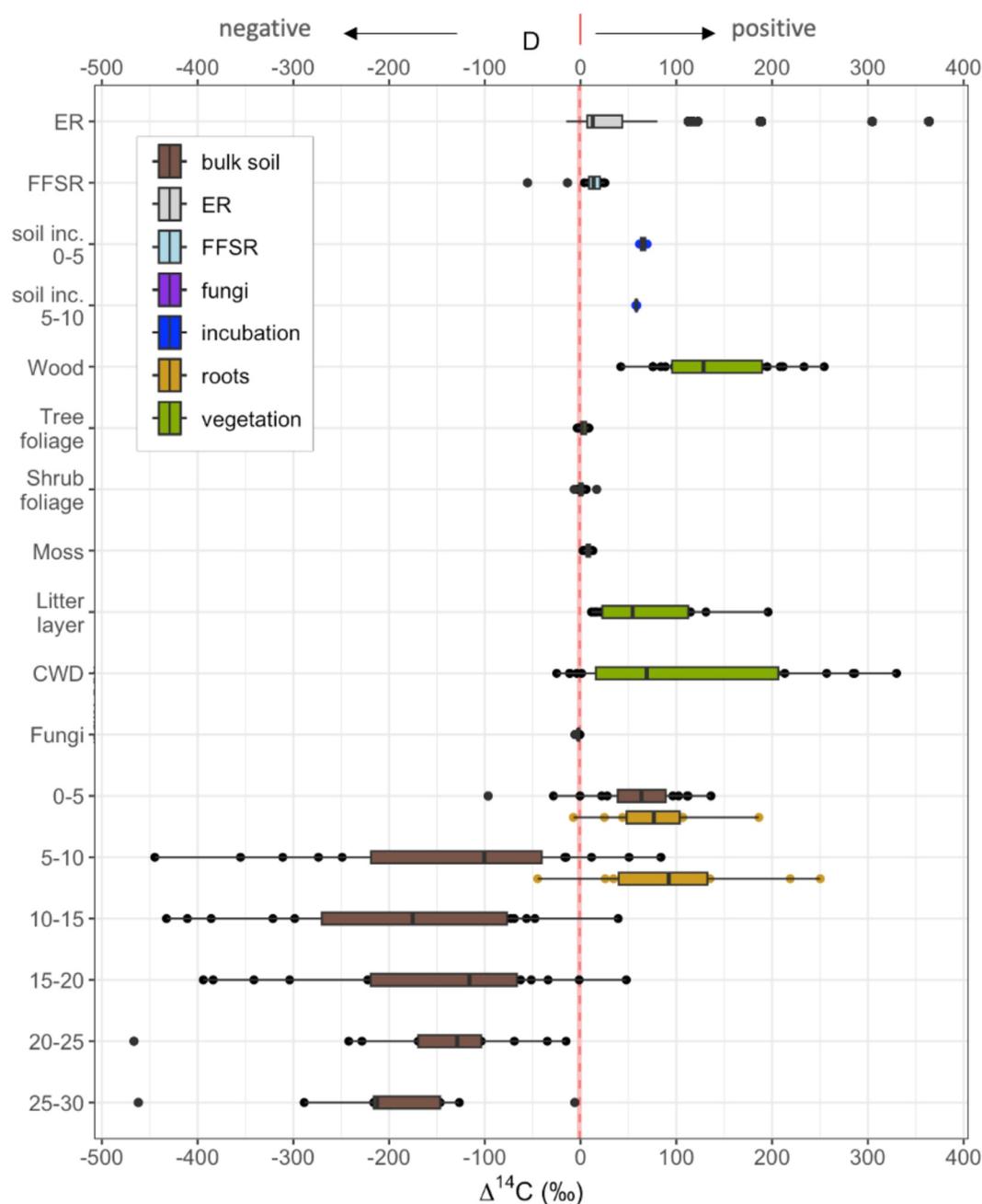
Figure 4. $\Delta^{14}C$ values from different ecosystem pools in bulk material and CO_2 fractions. Bulk soil is presented from 0 to 30 cm depths at 5 cm intervals. ER represents ecosystem respiration. Forest floor soil respiration values represent an average over 4 days of sampling. Soil incubation (soil inc.) and roots from the organic layer (0–5 cm) and the mineral soil (5–10 cm) are included. Atmospheric $^{14}C-CO_2$ is shown as a vertical dashed red line ($-2.3‰$) with associated uncertainty indicated by $\pm\sigma$. D at 0 indicates the boundary between positive and negative isotopic disequilibrium.

mineral soil (5–10 cm), amounting to 32.3% and 7.9%, respectively. Below a soil depth of 10 cm, the TOC concentration decreased to less than 3%.

Average $\Delta^{14}C$ value of background atmospheric CO_2 at 150-m height for August 2022 was $-2.3‰$ ($n = 4$). The radiocarbon composition of the different pools in the boreal forest stand varied from -466.5 to $329.9‰$ (Table 1). Most of the components had a wide range of variation and showed positive values of $\Delta^{14}C$, indicating post 1950 CO_2 incorporation (Figure 4). The analytical errors of ^{14}C measurements ranged from 1.4 to 2.9‰ for vegetation
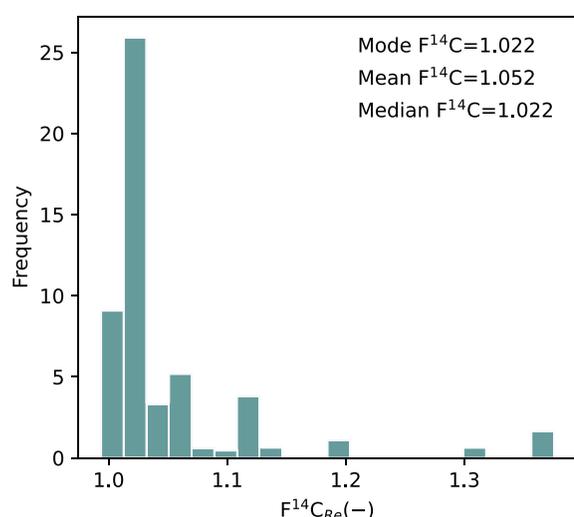
Figure 5. Histogram of frequencies with the slope values obtained from the bootstrap analysis representing the radiocarbon signature (in $F^{14}C$) of Re.

and root samples (mean = median = 2.1‰), and from 1.4 to 2.4‰ for soil solid samples (mean = median = 1.9‰). Soil respiration errors varied between 2.1 and 3.8‰ (mean = 3‰; median = 3.3‰), while soil incubations showed errors from 1.6 to 2.0‰ (mean = median = 1.8‰). Errors for atmospheric and ambient air ranged from 1.9 to 3.1‰ (mean = median = 2.1‰).

3.1. $\Delta^{14}C$ From Vegetation Pools, Fungi and Soil Profiles

Vegetation pools showed a positive D compared to the atmospheric background indicating an enrichment in bomb C. Mean $\Delta^{14}C$ values of live biomass such as in shrub foliage (1.2‰), tree foliage (2.9‰) and moss (7.8‰) showed a high significant difference among their means (p-value < 0.001), except for tree foliage versus shrub foliage (p-value = 0.341). $\Delta^{14}C$ values of live biomass pools were significantly different than the atmospheric background mean (p-values < 0.01). In contrast, $\Delta^{14}C$ values of wood (140.7‰) and dead biomass pools such as litter layer (68.4‰) and CWD (105.2‰) presented a wide range of variation although with no significant difference between the means of litter layer versus CWD (p-value = 0.326) and wood versus CWD (p-value = 0.349). Roots had positive D and presented wide variation in $\Delta^{14}C$ values. The mean $\Delta^{14}C$ of roots in the 0–5 cm layer (77.0‰) was not statistically different than that value of roots in the 5–10 cm layer (98.4‰) (p-value = 0.528). The $\Delta^{14}C$ value in fruiting bodies of mycorrhizal fungi was in equilibrium with the atmosphere with no significant difference (p-value = 0.833).

Soil layers showed generally a wide variability in their $\Delta^{14}C$ values. Only the soil organic layer had a positive D with a mean $\Delta^{14}C$ of 55.6‰ indicating significant difference (p-value < 0.001) with the rest of the soil depths. Soil layers had a significantly negative D compared with the atmosphere (p-value < 0.01) but similar among themselves (p-value > 0.005), and although the mean $\Delta^{14}C$ bulk values are not consistently decreasing with depth, the most depleted measurements were found in the horizons 20–25 (−466.5‰) and 25–30 cm (−461.9‰). Nonetheless, upper layers (above 15 cm) also contain extremely depleted $\Delta^{14}C$ values reaching −444.7‰.

3.2. $\Delta^{14}C$-CO_2 From Incubation and FFSR

The mean $\Delta^{14}C$ values of CO_2 from incubated soils showed significant differences among the organic and the mineral layers (p-value = 0.025). The organic layer was slightly more enriched in bomb C (65.3‰, $\sigma = 3.6$) than mineral soil layer below (58.3‰, $\sigma = 0.7$). Mean $\Delta^{14}C$ from FFSR (8.5‰, $\sigma = 20.9$) was significantly different from the atmospheric air (p-value = 0.024), but fell relatively close to equilibrium (Figure A4). However, $\Delta^{14}C$-CO_2 presented diurnal variation with a tendency toward more depleted values for the time integration comprising night-time respiration (−13.7‰ at 01:30 and −55.4‰ at 19:30). These depleted values were more remarkable in chamber 2. From the 24 samples of FFSR, only 14 were successfully extracted in the lab and therefore the diurnal cycle could not be fully completed for any of the chambers.

3.3. $\Delta^{14}C$ of Total Ecosystem Respiration

The slope of the regression between ΔCO_2 and $\Delta(F^{14}C \times CO_2)$ using the collected data from the six different heights indicated the predominant isotopic signature for the total Re. The results of applying the Miller-Tans approach provided a median value of slope of 1.02157 in F^{14} notation (Figure 5), which is equivalent to a mean of 42.8‰ and a median of 12.7‰ in $\Delta^{14}C$ notation (see Table 1). Although the values range from very depleted to very enriched $\Delta^{14}C$, the median better describes the most predominant radiocarbon signature.

4. Discussion

4.1. D in Bulk Material of Boreal Forest Pools

In general, $\Delta^{14}C$ from live biomass such as foliage and moss showed a low positive D close to equilibrium with

the atmospheric ^{14}C concentration. This low difference indicates that these pools fix modern C from the atmosphere, but store it mainly for short timescales behaving as fast-cycling pools. In contrast, roots, wood, CWD and litter layer presented positive D with enrichment in bomb C indicating fast to intermediate timescales of C cycling. The large variability in the Δ^{14}C values of the litter layer and CWD pools indicate that they are composed by a mixture of organic matter from different sources that results in distinct decomposition rates and ^{14}C content. For example, CWD can consist of both old and recent biomass formed by C fixed in the order of one year to several decades, potentially pre-dating the assumed age range of the forest stand (110 years). Largely, all the vegetation pools contained mostly bomb C, indicating that these pools cycle C in annual to decadal timescales. It was possible, however, to observe pre-bomb C in CWD, which may be interpreted as C legacies of dead biomass from a previous forest. The mean Δ^{14}C values in the roots aligns with previously observed fine root ages in boreal forests, which range between 2 and 12 years (Solly et al., 2018). However, the presence of values suggesting C ages exceeding 2 decades could be attributed to several factors: the addition of C from storage (Sah et al., 2011), an increase in C age in mineral and less fertile soils (Sah et al., 2013), or the presence of dead roots skewing the age distribution.

C in fungal fruiting bodies registered the closest ^{14}C signature to the current atmosphere, indicating the incorporation of the youngest available atmospheric CO_2. It is interesting to note that Δ^{14}C values in mycorrhizal fungi showed younger C than in vegetation pools, suggesting a rapid transport and allocation of C after photosynthesis. The use of different C sources depends on the fungal associations: on the one hand mycorrhizal fungi would register a short transit time (Suetsugu et al., 2020) with ages between 0 and 2 years (Hobbie et al., 2002); on the other hand, wood decomposers would incorporate C with ages from 1 to 30 years (Hobbie et al., 2020; Suetsugu et al., 2020). In this sense, the variability in C composition in fungal biomass depends on fungal ecology and, specifically for saprotrophic fungi, on the decomposed substrate (Hattae et al., 2020). For the first case, the influence of mixotrophic plants which mix their own photosynthetic C and fungal C (Selosse et al., 2017) may confound the final Δ^{14}C value in fungal fruiting bodies that in turn take C through the mycorrhizal network. Understanding the C dynamics within fungal biomass and their interdependent partners provides valuable insights with respect to recent C cycling, especially in Swedish forests where Lindahl et al. (2021) found that the C storage in the organic topsoil was 33% less in the presence of a species of ectomycorrhizal fungi.

The mineral soil presented mostly negative D with highly depleted Δ^{14}C values ($< -400‰$), indicating significant radioactive decay and slow-cycling pools with minimal atmospheric C incorporation since the 1950s (Schuur et al., 2023). Therefore, most soil organic carbon has persisted for millennia, but not older than the last glacial retreat (10,200 years BP) (Stroeven et al., 2016). Soil layers at 5–20 cm depth contained lesser quantities of bomb C, with very depleted Δ^{14}C values between 5 and 15 cm. Notably, the Δ^{14}C content did not decrease continuously with soil depth as previously found in archived soils (Torn et al., 2002; von Fromm et al., 2024). The presence of bomb C in deep soil layers suggests contributions of root-derived carbon in mineral soil (Rasse et al., 2005). Processes such as cryoturbation (Erdbrügger et al., 2023) and dissolved organic carbon (DOC) mobilization to deeper soil layers likely contribute to C stabilization in glacial sediments. However, new C introduced to the mineral soil does not necessarily stabilize in slow-cycling pools. This conclusion is supported by findings that about 34% of the extracted DOC from Krycklan catchment podzols is old C, with an average age of around 1,000 years (Hensgens et al., 2021).

Δ^{14}C values in the organic soil layer presented a positive D due to the presence of bomb C from the contribution of litter material since the last century. The organic layer, approximately 5 cm thick, has a distinctly different range of Δ^{14}C values compared to the mineral soil, suggesting contrasting soil formation conditions and negligible SOM accumulation rates in the mineral soil. The drastic drop in TOC content below the organic layer indicates that SOM accumulation was almost negligible before the forest was protected.

4.2. D From FFSR Reveals Diurnal Variability and Alternation Between Fast and Slow Pools

FFSR showed a positive D (mean = 8.5‰) although relatively close to equilibrium with the atmosphere, suggesting that the respired C is younger than the C stored in its sources (CWD, litter layer, soil at 0–10 cm depth, and roots). More negative Δ^{14}C values at night suggest a shift from autotrophic respiration in the morning to heterotrophic respiration at night, indicating a change from fast-cycling to slow-cycling pools. FFSR negative Δ^{14}C values might also indicate the contribution from C sources stored for longer times, like from mosses that fix soil

respired CO_2, deeper soil layers or even from root-derived respiration from a source reflecting atmospheric $\Delta^{14}C$ from previous years (Schuur & Trumbore, 2006) like in chamber 2. Hence, we interpret that FFSR comes from a mix of root-soil respiration and decomposition of post-bomb labile SOM derived from foliage, moss, litter layer and CWD (Gaudinski et al., 2000; Rodeghiero et al., 2013), typical in boreal soils (Anderson, 1992; Valentini et al., 2000).

4.3. Released CO_2 From Incubated Soils and Total Ecosystem Respiration Is Dominated by Young C

Respired $\Delta^{14}CO_2$ mean values from incubated soil differed significantly between the two depth intervals. Despite organic matter accumulation since the forest protection, the $\Delta^{14}C$ signature of respired CO_2 from soil incubations was predominantly bomb C. In the organic layer (0–5 cm), the released $\Delta^{14}CO_2$ aligns with the mean bulk $\Delta^{14}C$ and suggests the decomposition of recently accumulated post-bomb C. Contrarily, within the 5–10 cm layer, where pre-bomb C predominates, only the most readily decomposable C is being respired. This is indicated by the similarity between the mean $\Delta^{14}CO_2$ and the highest $\Delta^{14}C$ bulk values for this depth. Hence, we can interpret that decomposers metabolize C of similar age independently of the heterogeneous composition of the substrate.

The presence of small amounts of bomb C in deep soil horizons is indicative that root growth and other mechanisms of SOM mobilization have transported recent C downwards to the soil profile where C was generally much older (Gaudinski et al., 2000). Several studies have observed that freshly assimilated C from plants is rapidly transported and selectively utilized for below-ground soil respiration, particularly from the late morning hours onwards (Bahn et al., 2009). Conversely, photosynthates from previous days are predominant as a respiration substrate during the nocturnal and early morning periods (Bahn et al., 2009). Depending on the transit time of organic matter in the soil and the relative contribution of root respiration to the total CO_2 production, the ^{14}C content will be more or less different from the atmosphere (Carbone et al., 2008; Czimczik et al., 2006; Dörr & Münnich, 1986). The variation of turnover times and distribution of C stocks has been observed to be modulated by climate, edaphic, biological and hydrological variables (Hopkins et al., 2014; McFarlane et al., 2013) as well as soil frost (Muhr et al., 2009). In the boreal forest, below-canopy atmospheric CO_2 typically exhibits a positive D close to the background atmosphere, reflecting the decomposition of SOM enriched after nuclear weapon testing (Koarashi et al., 2002, 2004) and suggesting that the ecosystem is not releasing old C into the atmosphere.

The calculated range of $\Delta^{14}C$ values for total Re reveals its composite signature originating from various pools within the boreal forest. The results of our model indicated that the median value (12.7‰) captures the most common ^{14}C signature from the atmospheric mixture below the canopy, with a reduced emphasis on the outliers likely originating from C respired during the night or from intermediate to slow cycling pools. Furthermore, dead biomass and the organic layer contributed to the overall respiration flux, although to a lesser degree, as recorded by the high $\Delta^{14}C$ values captured in wood, litter layer, CWD and roots. This median Re value, similar to the FFSR, underscores the significance of live biomass pools (tree foliage, shrub foliage and moss) as a contemporary source of CO_2 and as the main inputs during the peak of the growing season in August. We infer that soil layers below 20 cm depth did not contribute to the total Re given the absence of negative $\Delta^{14}C$ values. All together, the respiration flux from the SVB forest primarily comprises C fixed within days to decades, with minimal presence of C captured before the nuclear era. This implies that the SVB forest is actively cycling recent C that spent days to years since fixation. However, it is essential to acknowledge that both the $\Delta^{14}C$ signature of total Re and its D are dependent on seasonal variations and changing meteorological conditions (Pedron et al., 2022; Phillips et al., 2013).

4.4. C Storage and Implications for C Sequestration

TOC is mainly confined to the organic layer, situated above the boundary with the sandy-silty soils developed on till sediments (Erlandsson Lampa et al., 2020; Laudon et al., 2021) at a depth of 10 cm. The steep decline in TOC in the mineral soil has been already found in the nordic forests (Callesen et al., 2003). This points to a notably slow accumulation rate of SOM, as the organic layer has only reached a thickness around 5 cm. Our observations suggest that post-bomb CO_2 absorbed through photosynthesis, primarily resides within the organic layer. The little amount of bomb C and TOC in deep soil layers implies that recent C enters the mineral soil to a limited extent. While stabilization of SOM may be taking place throughout the soil profile, there is no indication of significant new C stored below 10 cm depth. Therefore, storing C in boreal forest soils may not be very efficient as

a climate change mitigation strategy in the short-term due to the fact that most of the C entering the system might be respired back to the atmosphere within the first year (Carbone et al., 2008; Sierra et al., 2023). A recent labeling experiment conducted by Liebmann et al. (2022) found that one third of the litter C applied to forest soils was quickly mineralized and released into the atmosphere, while another third remained at the surface even after 2 years, establishing a difference between the theoretical C storage capacity of subsoils determined in laboratory settings and the actual C sequestration observed in natural environments. Even though the age of C in the subsoil might increase with depth, indicated by the depleted $\Delta^{14}C$ values, TOC content appears in very small quantities.

Accurate quantification of soil C stocks in our study is limited by the lack of in situ bulk density (BD) measurements for the specific soil layers sampled. However, previous studies have used pedotransfer functions to estimate BD for the Krycklan catchment (Larson et al., 2023; Martínez-García et al., 2022) and coarse sampling for the northern boreal forest (Callesen et al., 2003; Harrison et al., 2000; Olsson et al., 2009). The precision of these estimates varies with site characteristics (Dalsgaard et al., 2016), resulting in significant uncertainties in soil C calculations (Vanguelova et al., 2016). To illustrate, Larson et al. (2023) found that total C stocks are widely variable in the Krycklan catchment, mainly correlating to soil moisture, a soil parameter we did not obtain. Although total soil C stocks (excluding peat) estimates (67 Mg C ha^{-1}) indicate that most of it is contained in the mineral C pool (40 Mg C ha^{-1}) (Larson et al., 2023), this fraction is not as dynamic or biologically active as the organic C, which has been found to play a more direct role in supporting microbial activity, nutrient cycling, and therefore in CO_2 production. Our estimate of soil C stocks for the organic layer, with a BD of 0.07 g cm^{-3} (Harrison et al., 2000), was 11.3 Mg C ha^{-1}, which matches the stocks reported by Harrison et al. (2000) for Å heden in North Sweden. For the mineral soil, we calculated the stocks using an average BD of 0.85 g cm^{-3} ($\sigma = 0.07$), as reported for the Krycklan catchment (Martínez-García et al., 2022). The calculated stocks were 45 and 66.8 Mg C ha^{-1} for a depth to 20 cm and 30 cm, respectively, which align closely with the findings of Larson et al. (2023).

The capacity of the boreal forest ecosystems to stabilize SOM is then hindered by the relative low net primary productivity (NPP) allocated belowground (Saugier et al., 2001; Xiao et al., 2023) and by the fact that a large proportion of the recent C inputs is used by microorganisms (Bernard et al., 2022; Högberg et al., 2001; Scheibe et al., 2023). In addition to that, lateral C fluxes from biomass harvest and C export to rivers account for an important share of NPP unable to be fixed as C stocks (Ciais et al., 2021), adding more uncertainty to the capacity of boreal forest to sequester atmospheric CO_2. Nevertheless, recent studies have shown that boreal forests have behaved as a C sink in recent years (Chi et al., 2019, 2020; Yang et al., 2023), with higher proportions of C uptake observed in managed forests compared to low-intensive and unmanaged ones (Peichl et al., 2023). For example, Peichl et al. (2023) found that NPP in the boreal biome strongly depended on intrinsic landscape characteristics, which posits the challenge of acquiring more detailed mesoscale empirical data in order to understand its C sink capacity.

Sustainable C sequestration strategies must focus on stimulating the stabilization of new inputs of CO_2 into slow-cycling reservoirs. To measure how long and how much new C remains in the different pools, the use of D and comprehensive C content measurements along with metrics that integrate the time it remains in storage, such as age and transit time (Muñoz et al., 2023; Sierra et al., 2017, 2021) are essential. Overall, although the boreal biome has shown to store significant amounts of C in managed forest during the last years, it is imperative to further understand the timescales of C allocation in tree biomass and soils to better inform climate change mitigation measures.

5. Conclusions

The end of the radiocarbon bomb period in the atmosphere of the northern hemisphere provided an opportunity to evaluate the degree of new C incorporation in a boreal forest ecosystem by calculating the D in different pools as summarized in Figure 6.

We have presented a comprehensive analysis of the radiocarbon D in a wide range of pools of a boreal forest ecosystem, contributing to understanding the allocation of C and timescales of C cycling. Our results indicate that, on the one hand, C presents fast cycling rates (months to years) in live biomass and intermediate cycling rates (years to decades) in dead biomass and wood. On the other hand, mineral soils showed little incorporation of recent C from the atmosphere. Total ecosystem respiration and FFSR were predominantly close to equilibrium
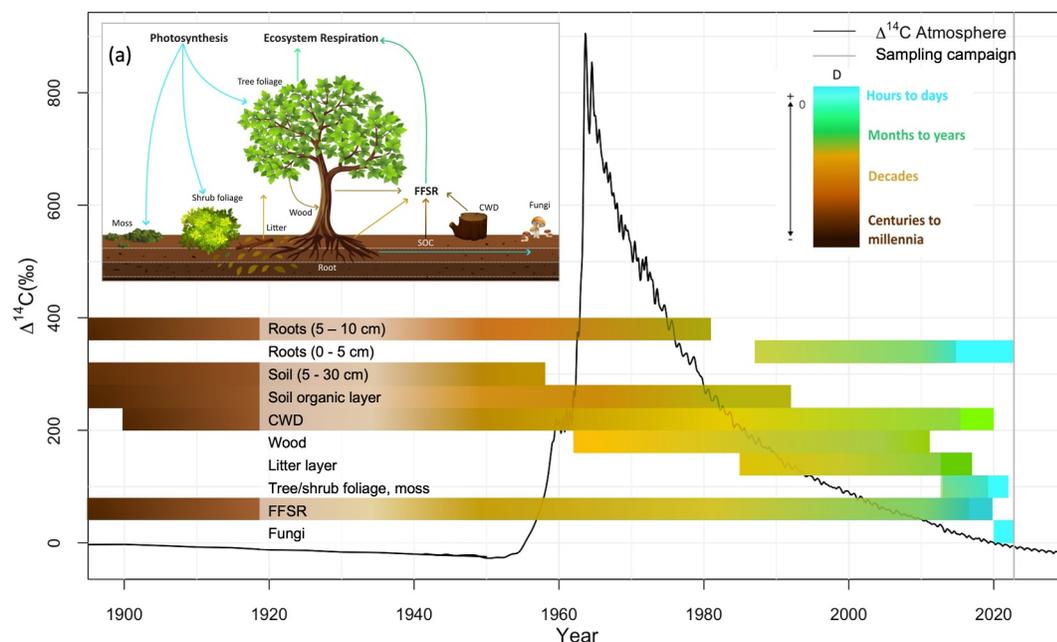
Figure 6. Representation of the timescales at which different components of the boreal forest integrate the ^{14}C atmospheric signal as CO_2, indicated by a color ramp. a) Components of the boreal forest and their interactions showing the *D*. Lines represent the direction of C transfers, colored based on their Δ^{14}C values, reflecting the *D* values for 2022.

with the atmosphere, suggesting that the output flux is dominated by autotrophic respiration of recently fixed and post-bomb labile C.

Altogether, we show evidence of a slow accumulation rate of SOM restricted to the most superficial soil layer, which coupled with the fast ecosystem respiration, indicates that boreal forests soils may not be efficient for short-term C sequestration. Although the boreal forest stores significant amounts of C, most of it is cycled in the order of days to decades from vegetation and the soil organic layer. Only minimal amounts of new C are incorporated and stabilized over long timescales. The capacity of the boreal forest soils to store C in the mineral soil is then limited by the relatively low NPP allocated belowground (Saugier et al., 2001; Xiao et al., 2023) and the large proportion of C inputs used by microorganisms (Bernard et al., 2022; Högberg et al., 2001; Scheibe et al., 2023). While the boreal biome has been a net C sink in recent decades, further understanding of its C cycling timescales is needed, particularly for better informed decisions on climate change mitigation measures.

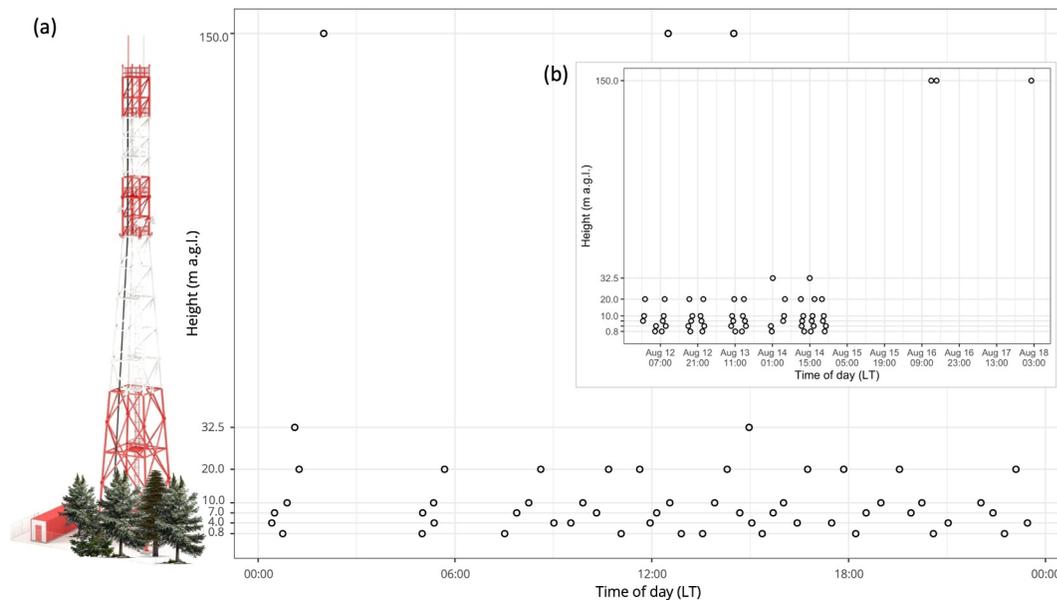## Appendix A: Additional Information on Sampling and TOC Results

Figure A1. Time and height distribution of atmospheric air sampling from the Svarberget research station grouped by time of the day (a) and over the sampling dates (b).
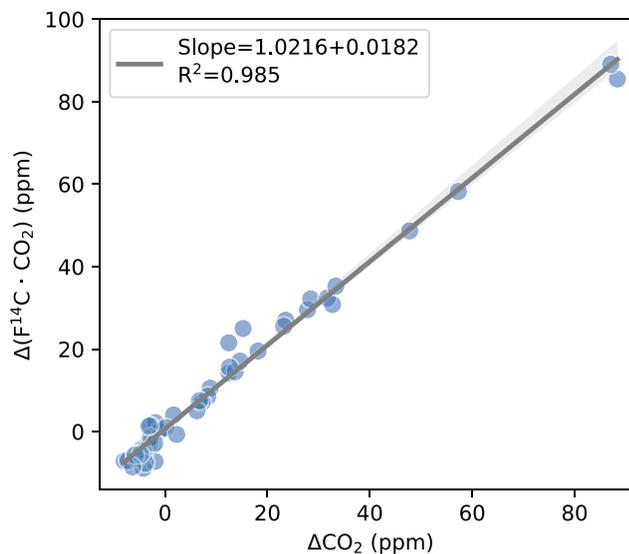

Figure A2. Example of one regression between ΔCO_2 and $\Delta(F^{14}C \cdot CO_2)$ using the Miller-Tans plot to obtain the slope as an estimate of the radiocarbon signature of (Re). These regressions were repeated 50,000 times randomly selecting the set of points to obtain an estimate of uncertainty.
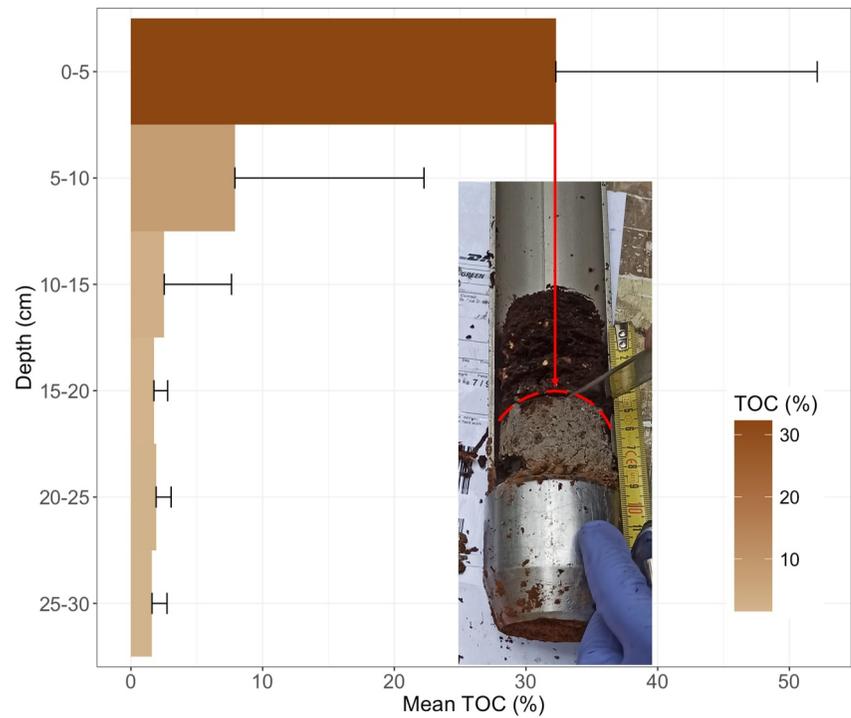
Figure A3. Mean total organic carbon percentage at different depths in the soil profile. Error lines represent one σ above the mean. The red line shows the boundary between the organic layer and the sandy-silty mineral soil layers. It is important to note that this boundary was not consistently positioned at a depth of 5 cm below the surface but exhibited spatial variability.
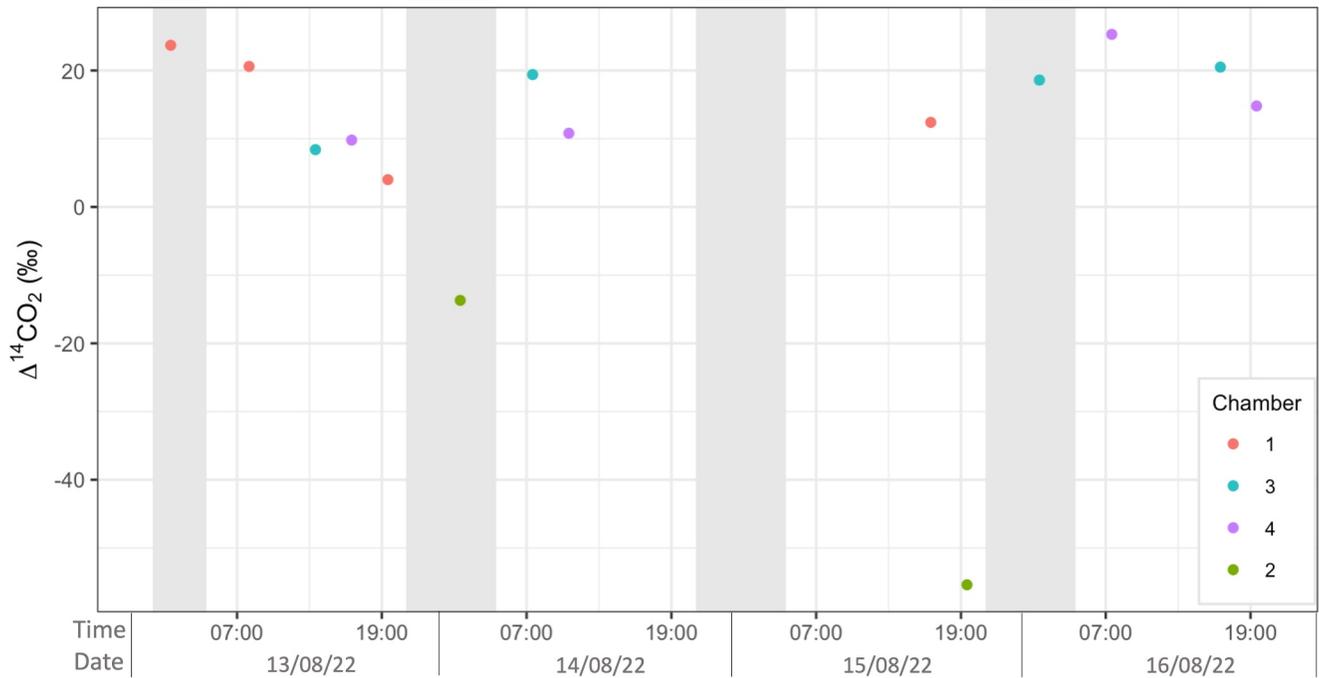

Figure A4. Diurnal variation of $\Delta^{14}CO_2$ from forest floor soil respiration along 4 days of sampling. Gray bars indicate nighttime. Average length of the day for the sampling dates was 16 hr and 32 m. Sunrise was at 04:29 and sunset at 21:01.

Table A1
Total Organic Carbon (%) Statistics for Each Measured Pool in the Boreal Forest Stand

Pool	Samples	Mean	Median	SD	Min.	Max.
Wood	5	50.73	50.47	0.72	50.10	51.94
Tree foliage	5	52.70	52.62	0.21	52.51	53.06
Shrub foliage	5	52.34	52.08	0.56	51.75	52.97
Moss	5	48.50	48.27	0.61	47.78	49.18
Litter layer	5	53.02	52.72	1.06	51.80	54.65
CWD	5	53.73	53.49	2.24	50.66	56.89
Fungi	6	48.21	48.63	1.50	45.82	49.87
Soil 0–5	19	32.27	36.63	19.85	3.86	55.40
Soil 5–10	20	7.89	2.20	14.36	0.40	56.43
Soil 10–15	20	2.53	1.21	5.10	0.48	23.90
Soil 15–20	19	1.74	1.37	1.04	0.48	3.91
Soil 20–25	13	1.91	1.42	1.14	0.75	5.01
Soil 25–30	9	1.60	1.15	1.14	0.55	3.92
Roots 0–5	10	49.15	49.38	1.66	45.18	51.23
Roots 5–10	10	41.37	46.19	9.65	24.95	50.03

Note. Second column indicates the number of samples used for the calculations. σ shows the standard deviation, and Min. and Max. indicate the minimum and maximum values within the evaluated range of data for each pool.

Data Availability Statement

Data supporting our study can be obtained from https://zenodo.org/records/10952030 (Tangarife-Escobar, Guggenberger, Feng, Muñoz, et al., 2024).

References

Alster, C. J., Allison, S. D., & Treseder, K. K. (2020). Carbon budgets for soil and plants respond to long-term warming in an Alaskan boreal forest. *Biogeochemistry*, *150*(3), 345–353. https://doi.org/10.1007/s10533-020-00697-0

Anderson, J. (1992). Responses of soils to climate change. In *Advances in ecological research* (Vol. 22, pp. 163–210). Elsevier. https://doi.org/10.1016/s0065-2504(08)60136-1

Bahn, M., Schmitt, M., Siegwolf, R., Richter, A., & Brüggemann, N. (2009). Does photosynthesis affect grassland soil-respired CO2 and its carbon isotope composition on a diurnal timescale? *New Phytologist*, *182*(2), 451–460. https://doi.org/10.1111/j.1469-8137.2008.02755.x

Balesdent, J. (1987). The turnover of soil organic fractions estimated by radiocarbon dating. *Science of the Total Environment*, *62*, 405–408. https://doi.org/10.1016/0048-9697(87)90528-6

Bernard, L., Basile-Doelsch, I., Derrien, D., Fanin, N., Fontaine, S., Guenet, B., et al. (2022). Advancing the mechanistic understanding of the priming effect on soil organic matter mineralisation. *Functional Ecology*, *36*(6), 1355–1377. https://doi.org/10.1111/1365-2435.14038

Betson, N. R., Göttlicher, S. G., Hall, M., Wallin, G., Richter, A., & Högberg, P. (2007). No diurnal variation in rate or carbon isotope composition of soil respiration in a boreal forest. *Tree Physiology*, *27*(5), 749–756. https://doi.org/10.1093/treephys/27.5.749

Bowling, D., Ballantyne, A. P., Miller, J., Burns, S., Conway, T., Menzer, O., et al. (2014). Ecological processes dominate the ^{13}C land disequilibrium in a rocky mountain subalpine forest. *Global Biogeochemical Cycles*, *28*(4), 352–370. https://doi.org/10.1002/2013gb004686

Bradshaw, C. J., & Warkentin, I. G. (2015). Global estimates of boreal forest carbon stocks and flux. *Global and Planetary Change*, *128*, 24–30. https://doi.org/10.1016/j.gloplacha.2015.02.004

Callesen, I., Liski, J., Raulund-Rasmussen, K., Olsson, M., Tau-Strand, L., Vesterdal, L., & Westman, C. (2003). Soil carbon stores in nordic well-drained forest soils—Relationships with climate and texture class. *Global Change Biology*, *9*(3), 358–370. https://doi.org/10.1046/j.1365-2486.2003.00587.x

Carbone, M. S., Winston, G. C., & Trumbore, S. E. (2008). Soil respiration in perennial grass and shrub ecosystems: Linking environmental controls with plant and microbial sources on seasonal and diel timescales. *Journal of Geophysical Research*, *113*(G2). https://doi.org/10.1029/2007jg000611

Chi, J., Nilsson, M. B., Kljun, N., Wallerman, J., Fransson, J. E., Laudon, H., et al. (2019). The carbon balance of a managed boreal landscape measured from a tall tower in northern Sweden. *Agricultural and Forest Meteorology*, *274*, 29–41. https://doi.org/10.1016/j.agrformet.2019.04.010

Chi, J., Nilsson, M. B., Laudon, H., Lindroth, A., Wallerman, J., Fransson, J. E., et al. (2020). The net landscape carbon balance—Integrating terrestrial and aquatic carbon fluxes in a managed boreal forest landscape in Sweden. *Global Change Biology*, *26*(4), 2353–2367. https://doi.org/10.1111/gcb.14983

Ciais, P., Yao, Y., Gasser, T., Baccini, A., Wang, Y., Lauerwald, R., et al. (2021). Empirical estimates of regional carbon budgets imply reduced global soil heterotrophic respiration. *National Science Review*, *8*(2), nwaa145. https://doi.org/10.1093/nsr/nwaa145

Crow, S. E., & Sierra, C. A. (2022). The climate benefit of sequestration in soils for warming mitigation. *Biogeochemistry*, *161*(1), 71–84. https://doi.org/10.1007/s10533-022-00981-1

Czimczik, C. I., Trumbore, S. E., Carbone, M. S., & Winston, G. C. (2006). Changing sources of soil respiration with time since fire in a boreal forest. *Global Change Biology*, *12*(6), 957–971. https://doi.org/10.1111/j.1365-2486.2006.01107.x

Dalsgaard, L., Lange, H., Strand, L. T., Callesen, I., Borgen, S. K., Liski, J., & Astrup, R. (2016). Underestimation of boreal forest soil carbon stocks related to soil classification and drainage. *Canadian Journal of Forest Research*, *46*(12), 1413–1425. https://doi.org/10.1139/cjfr-2015-0466

De Camargo, P. B., Trumbore, S. E., Martinelli, L. A., Davidson, E. A., Nepstad, D. C., & Victoria, R. L. (1999). Soil carbon dynamics in regrowing forest of eastern Amazonia. *Global Change Biology*, *5*(6), 693–702. https://doi.org/10.1046/j.1365-2486.1999.00259.x

Dörr, H., & Münnich, K. (1986). Annual variations of the ^{14}C content of soil CO_2. *Radiocarbon*, *28*(2A), 338–345. https://doi.org/10.1017/s0033822200007438

Drought 2018 Team and ICOS Atmosphere Thematic Centre. (2020). Drought-2018 atmospheric CO_2 mole fraction product for 48 stations (96 sample heights). *ICOS ERIC - Carbon Portal*. https://doi.org/10.18160/ERE9-9D85

Eglinton, T. I., Graven, H. D., Raymond, P. A., Trumbore, S. E., Aluwihare, L., Bard, E., et al. (2023). Making the case for an international decade of radiocarbon. *Philosophical Transactions of the Royal Society A: Mathematical, Physical & Engineering Sciences*, *381*(2261), 20230081. https://doi.org/10.1098/rsta.2023.0081

Erdbrügger, J., van Meerveld, I., Seibert, J., & Bishop, K. (2023). Shallow-groundwater-level time series and a groundwater chemistry survey from a boreal headwater catchment, Krycklan, Sweden. *Earth System Science Data*, *15*(4), 1779–1800. https://doi.org/10.5194/essd-15-1779-2023

Erlandsson Lampa, M., Sverdrup, H. U., Bishop, K. H., Belyazid, S., Ameli, A., & Köhler, S. J. (2020). Catchment export of base cations: Improved mineral dissolution kinetics influence the role of water transit time. *Soil*, *6*(1), 231–244. https://doi.org/10.5194/soil-6-231-2020

Fung, I., Field, C., Berry, J., Thompson, M., Randerson, J., Malmström, C., et al. (1997). Carbon 13 exchanges between the atmosphere and biosphere. *Global Biogeochemical Cycles*, *11*(4), 507–533. https://doi.org/10.1029/97gb01751

Garnett, M. H., Newton, J.-A., & Parker, T. C. (2021). A highly portable and inexpensive field sampling kit for radiocarbon analysis of carbon dioxide. *Radiocarbon*, *63*(4), 1355–1368. https://doi.org/10.1017/rdc.2021.49

Gaudinski, J. B., Trumbore, S. E., Davidson, E. A., & Zheng, S. (2000). Soil carbon cycling in a temperate forest: Radiocarbon-based estimates of residence times, sequestration rates and partitioning of fluxes. *Biogeochemistry*, *51*(1), 33–69. https://doi.org/10.1023/a:1006301010014

Harrison, A., Harkness, D., Rowland, A., Garnett, J., & Bacon, P. (2000). Annual carbon and nitrogen fluxes in soils along the European forest transect, determined using ^{14}C-bomb. In *Carbon and nitrogen cycling in european forest ecosystems* (pp. 237–256). Springer.

Hattae, C., Zazzo, A., & Selosse, M.-A. (2020). The radiocarbon age of mycoheterotrophic plants. *New Phytologist*, *227*(5), 1284–1288. https://doi.org/10.1111/nph.16637

Heimann, M., Jordan, A., Brand, W., Lavric, J., Moossen, H., & Rothe, M. (2022). Atmospheric flask sampling program of MPI-BGC, version 13, January, 2022. Edmond. https://doi.org/10.17617/3.8r

Hensgens, G., Laudon, H., Johnson, M. S., & Berggren, M. (2021). The undetected loss of aged carbon from boreal mineral soils. *Scientific Reports*, *11*(1), 6202. https://doi.org/10.1038/s41598-021-85506-w

Hobbie, E. A., Grandy, A. S., & Harmon, M. E. (2020). Isotopic and compositional evidence for carbon and nitrogen dynamics during wood decomposition by saprotrophic fungi. *Fungal Ecology*, *45*, 100915. https://doi.org/10.1016/j.funeco.2020.100915

Hobbie, E. A., Weber, N. S., Trappe, J. M., & Van Klinken, G. J. (2002). Using radiocarbon to determine the mycorrhizal status of fungi. *New Phytologist*, *156*(1), 129–136. https://doi.org/10.1046/j.1469-8137.2002.00496.x

Högberg, P., Nordgren, A., Buchmann, N., Taylor, A. F., Ekblad, A., HoÈgberg, M. N., et al. (2001). Large-scale forest girdling shows that current photosynthesis drives soil respiration. *Nature*, *411*(6839), 789–792. https://doi.org/10.1038/35081058

Hopkins, F. M., Filley, T. R., Gleixner, G., Lange, M., Top, S. M., & Trumbore, S. E. (2014). Increased belowground carbon inputs and warming promote loss of soil organic carbon through complementary microbial responses. *Soil Biology and Biochemistry*, *76*, 57–69. https://doi.org/10.1016/j.soilbio.2014.04.028

Hua, Q., Turnbull, J. C., Santos, G. M., Rakowski, A. Z., Ancapichún, S., De Pol-Holz, R., et al. (2022). Atmospheric radiocarbon for the period 1950–2019. *Radiocarbon*, *64*(4), 723–745. https://doi.org/10.1017/rdc.2021.95

ICOS RI, Bergamaschi, P., Colomb, A., De Mazière, M., Emmenegger, L., Kubistin, D., et al. (2022). *ICOS atmosphere release 2022-1 of level 2 greenhouse gas mole fractions of CO_2, CH_4, N_2O, CO, meteorology and $^{14}CO_2$*. https://doi.org/10.18160/KCYX-HA35

Kasischke, E. S. (2000). Boreal ecosystems in the global carbon cycle. In *Fire, climate change, and carbon cycling in the boreal forest* (pp. 19–30). Springer.

Keeling, C. D. (1958). The concentration and isotopic abundances of atmospheric carbon dioxide in rural areas. *Geochimica et Cosmochimica Acta*, *13*(4), 322–334. https://doi.org/10.1016/0016-7037(58)90033-4

Keeling, C. D. (1961). The concentration and isotopic abundances of carbon dioxide in rural and marine air. *Geochimica et Cosmochimica Acta*, *24*(3–4), 277–298. https://doi.org/10.1016/0016-7037(61)90023-0

Keeling, C. D. (1979). The suess effect: 13carbon-14carbon interrelations. *Environment International*, *2*(4–6), 229–300. https://doi.org/10.1016/0160-4120(79)90005-9

Koarashi, J., Amano, H., Andoh, M., Iida, T., & Moriizumi, J. (2002). Estimation of $^{14}CO_2$ flux at soil-atmosphere interface and distribution of ^{14}C in forest ecosystem. *Journal of Environmental Radioactivity*, *60*(3), 249–261. https://doi.org/10.1016/s0265-931x(01)00084-4

Koarashi, J., Iida, T., Moriizumi, J., & Asano, T. (2004). Evaluation of ^{14}C abundance in soil respiration using accelerator mass spectrometry. *Journal of Environmental Radioactivity*, *75*(2), 117–132. https://doi.org/10.1016/j.jenvrad.2003.11.005

Kwon, M. J., Heimann, M., Kolle, O., Luus, K. A., Schuur, E. A., Zimov, N., et al. (2016). Long-term drainage reduces CO_2 uptake and increases CO_2 emission on a Siberian floodplain due to shifts in vegetation community and soil thermal characteristics. *Biogeosciences*, *13*(14), 4219–4235. https://doi.org/10.5194/bg-13-4219-2016

LaFranchi, B., McFarlane, K., Miller, J., Lehman, S., Phillips, C., Andrews, A., et al. (2016). Strong regional atmospheric ^{14}C signature of respired CO_2 observed from a tall tower over the midwestern United States. *Journal of Geophysical Research: Biogeosciences*, *121*(8), 2275–2295. https://doi.org/10.1002/2015jg003271

Lal, R., Monger, C., Nave, L., & Smith, P. (2021). The role of soil in regulation of climate. *Philosophical Transactions of the Royal Society B*, *376*(1834), 20210084. https://doi.org/10.1098/rstb.2021.0084

Larson, J., Wallerman, J., Peichl, M., & Laudon, H. (2023). Soil moisture controls the partitioning of carbon stocks across a managed boreal forest landscape. *Scientific Reports*, *13*(1), 14909. https://doi.org/10.1038/s41598-023-42091-4

Laudon, H., Hasselquist, E. M., Peichl, M., Lindgren, K., Sponseller, R., Lidman, F., et al. (2021). Northern landscapes in transition: Evidence, approach and ways forward using the Krycklan catchment study. *Hydrological Processes*, *35*(4), e14170. https://doi.org/10.1002/hyp.14170

Laudon, H., Taberman, I., Ågren, A., Futter, M., Ottosson-Löfvenius, M., & Bishop, K. (2013). The Krycklan catchment study—A flagship infrastructure for hydrology, biogeochemistry, and climate research in the boreal landscape. *Water Resources Research*, *49*(10), 7154–7158. https://doi.org/10.1002/wrcr.20520

Levin, I., Naegler, T., Kromer, B., Diehl, M., Francey, R., Gomez-Pelaez, A., et al. (2010). Observations and modelling of the global distribution and long-term trend of atmospheric $^{14}CO_2$. *Tellus B: Chemical and Physical Meteorology*, *62*(1), 26–46. https://doi.org/10.3402/tellusb.v62i1.16511

Liebmann, P., Mikutta, R., Kalbitz, K., Wordell-Dietrich, P., Leinemann, T., Preusser, S., et al. (2022). Biogeochemical limitations of carbon stabilization in forest subsoils. *Journal of Plant Nutrition and Soil Science*, *185*(1), 35–43. https://doi.org/10.1002/jpln.202100295

Lindahl, B. D., Kyaschenko, J., Varenius, K., Clemmensen, K. E., Dahlberg, A., Karltun, E., & Stendahl, J. (2021). A group of ectomycorrhizal fungi restricts organic matter accumulation in boreal forest. *Ecology Letters*, *24*(7), 1341–1351. https://doi.org/10.1111/ele.13746

Lu, X., Wang, Y.-P., Luo, Y., & Jiang, L. (2018). Ecosystem carbon transit versus turnover times in response to climate warming and rising atmospheric CO2 concentration. *Biogeosciences*, *15*(21), 6559–6572. https://doi.org/10.5194/bg-15-6559-2018

Lundmark, T., Bergh, J., Hofer, P., Lundström, A., Nordin, A., Poudel, B. C., et al. (2014). Potential roles of Swedish forestry in the context of climate change mitigation. *Forests*, *5*(4), 557–578. https://doi.org/10.3390/f5040557

Martínez-García, E., Nilsson, M. B., Laudon, H., Lundmark, T., Fransson, J. E., Wallerman, J., & Peichl, M. (2022). Overstory dynamics regulate the spatial variability in forest-floor CO_2 fluxes across a managed boreal forest landscape. *Agricultural and Forest Meteorology*, *318*, 108916. https://doi.org/10.1016/j.agrformet.2022.108916

Matthews, H. D., Zickfeld, K., Koch, A., & Luers, A. (2023). Accounting for the climate benefit of temporary carbon storage in nature. *Nature Communications*, *14*(1), 5485. https://doi.org/10.1038/s41467-023-41242-5

McFarlane, K. J., Torn, M. S., Hanson, P. J., Porras, R. C., Swanston, C. W., Callaham, M. A., & Guilderson, T. P. (2013). Comparison of soil organic matter dynamics at five temperate deciduous forests with physical fractionation and radiocarbon measurements. *Biogeochemistry*, *112*(1–3), 457–476. https://doi.org/10.1007/s10533-012-9740-1

Miller, J. B., & Tans, P. P. (2003). Calculating isotopic fractionation from atmospheric measurements at various scales. *Tellus B: Chemical and Physical Meteorology*, *55*(2), 207–214. https://doi.org/10.3402/tellusb.v55i2.16697

Muhr, J., Borken, W., & Matzner, E. (2009). Effects of soil frost on soil respiration and its radiocarbon signature in a Norway spruce forest soil. *Global Change Biology*, *15*(4), 782–793. https://doi.org/10.1111/j.1365-2486.2008.01695.x

Muñoz, E., Chanca, I., & Sierra, C. A. (2023). Increased atmospheric CO_2 and the transit time of carbon in terrestrial ecosystems. *Global Change Biology*, *29*(23), 6441–6452. https://doi.org/10.1111/gcb.16961

Muñoz, E., & Sierra, C. A. (2023). Deterministic and stochastic components of atmospheric CO_2 inside forest canopies and consequences for predicting carbon and water exchange. *Agricultural and Forest Meteorology*, *341*, 109624. https://doi.org/10.1016/j.agrformet.2023.109624

Naegler, T., & Levin, I. (2009). Biosphere-atmosphere gross carbon exchange flux and the $\delta^{13}CO_2$ and $\Delta^{14}CO_2$ disequilibria constrained by the biospheric excess radiocarbon inventory. *Journal of Geophysical Research*, *114*(D17). https://doi.org/10.1029/2008JD011116

Olsson, M. T., Erlandsson, M., Lundin, L., Nilsson, T., Nilsson, Å., Stendahl, J., et al. (2009). Organic carbon stocks in Swedish podzol soils in relation to soil hydrology and other site characteristics. *Silva Fennica*, *43*(2), 209–222. https://doi.org/10.14214/sf.207

Pavelka, M., Acosta, M., Kiese, R., Altimir, N., Brümmer, C., Crill, P., et al. (2018). Standardisation of chamber technique for CO_2, N_2O and CH_4 fluxes measurements from terrestrial ecosystems. *International Agrophysics*, *32*(4), 569–587. https://doi.org/10.1515/intag-2017-0045

Pedron, S. A., Welker, J., Euskirchen, E., Klein, E., Walker, J., Xu, X., & Czimczik, C. (2022). Closing the winter gap—Year-round measurements of soil CO_2 emission sources in arctic tundra. *Geophysical Research Letters*, *49*(6), e2021GL097347. https://doi.org/10.1029/2021gl097347

Peichl, M., Martínez-García, E., Fransson, J. E., Wallerman, J., Laudon, H., Lundmark, T., & Nilsson, M. B. (2023). Landscape-variability of the carbon balance across managed boreal forests. *Global Change Biology*, *29*(4), 1119–1132. https://doi.org/10.1111/gcb.16534

Phillips, C., McFarlane, K., Risk, D., & Desai, A. (2013). Biological and physical influences on soil $^{14}CO_2$ seasonal dynamics in a temperate hardwood forest. *Biogeosciences*, *10*(12), 7999–8012. https://doi.org/10.5194/bg-10-7999-2013

Phillips, C., McFarlane, K. J., LaFranchi, B., Desai, A. R., Miller, J. B., & Lehman, S. J. (2015). Observations of $^{14}CO_2$ in ecosystem respiration from a temperate deciduous forest in northern Wisconsin. *Journal of Geophysical Research: Biogeosciences*, *120*(4), 600–616. https://doi.org/10.1002/2014jg002808

Price, D., Peng, C., Apps, M., & Halliwell, D. (1999). Simulating effects of climate change on boreal ecosystem carbon pools in central Canada. *Journal of Biogeography*, *26*(6), 1237–1248. https://doi.org/10.1046/j.1365-2699.1999.00332.x

Randerson, J., Enting, I., Schuur, E., Caldeira, K., & Fung, I. (2002). Seasonal and latitudinal variability of troposphere $\delta^{14}CO_2$: Post bomb contributions from fossil fuels, oceans, the stratosphere, and the terrestrial biosphere. *Global Biogeochemical Cycles*, *16*(4), 59-1–59-19. https://doi.org/10.1029/2002gb001876

Rasse, D. P., Rumpel, C., & Dignac, M.-F. (2005). Is soil carbon mostly root carbon? Mechanisms for a specific stabilisation. *Plant and Soil*, *269*(1–2), 341–356. https://doi.org/10.1007/s11104-004-0907-y

Reimer, P. J., Bard, E., Bayliss, A., Beck, J. W., Blackwell, P. G., Ramsey, C. B., et al. (2013). Intcal13 and marine13 radiocarbon age calibration curves 0–50,000 years cal bp. *Radiocarbon*, *55*(4), 1869–1887. https://doi.org/10.2458/azu_js_rc.55.16947

Rodeghiero, M., Churkina, G., Martinez, C., Scholten, T., Gianelle, D., & Cescatti, A. (2013). Components of forest soil CO_2 efflux estimated from δ ^{14}C values of soil organic matter. *Plant and Soil*, *364*(1–2), 55–68. https://doi.org/10.1007/s11104-012-1309-1

Sah, S. P., Bryant, C., Leppälammi-Kujansuu, J., Lõhmus, K., Ostonen, I., & Helmisaari, H.-S. (2013). Variation of carbon age of fine roots in boreal forests determined from ^{14}C measurements. *Plant and Soil*, *363*(1–2), 77–86. https://doi.org/10.1007/s11104-012-1294-4

Sah, S. P., Jungner, H., Oinonen, M., Kukkola, M., & Helmisaari, H.-S. (2011). Does the age of fine root carbon indicate the age of fine roots in boreal forests? *Biogeochemistry*, *104*(1–3), 91–102. https://doi.org/10.1007/s10533-010-9485-7

Saugier, B., Roy, J., & Mooney, H. A. (2001). Estimations of global terrestrial productivity. In *Terrestrial global productivity* (pp. 543–557).

Scheibe, A., Sierra, C. A., & Spohn, M. (2023). Recently fixed carbon fuels microbial activity several meters below the soil surface. *Biogeosciences*, *20*(4), 827–838. https://doi.org/10.5194/bg-20-827-2023

Schuur, E. A., Hicks Pries, C., Mauritz, M., Pegoraro, E., Rodenhizer, H., See, C., & Ebert, C. (2023). Ecosystem and soil respiration radiocarbon detects old carbon release as a fingerprint of warming and permafrost destabilization with climate change. *Philosophical Transactions of the Royal Society A*, *381*(2261), 20220201. https://doi.org/10.1098/rsta.2022.0201

Schuur, E. A., & Trumbore, S. E. (2006). Partitioning sources of soil respiration in boreal black spruce forest using radiocarbon. *Global Change Biology*, *12*(2), 165–176. https://doi.org/10.1111/j.1365-2486.2005.01066.x

Selosse, M.-A., Charpin, M., & Not, F. (2017). Mixotrophy everywhere on land and in water: The grand écart hypothesis. *Ecology Letters*, *20*(2), 246–263. https://doi.org/10.1111/ele.12714

Sierra, C. A., Estupinan-Suarez, L. M., & Chanca, I. (2021). The fate and transit time of carbon in a tropical forest. *Journal of Ecology*, *109*(8), 2845–2855. https://doi.org/10.1111/1365-2745.13723

Sierra, C. A., Hoyt, A. M., He, Y., & Trumbore, S. E. (2018). Soil organic matter persistence as a stochastic process: Age and transit time distributions of carbon in soils. *Global Biogeochemical Cycles*, *32*(10), 1574–1588. https://doi.org/10.1029/2018gb005950

Sierra, C. A., Müller, M., Metzler, H., Manzoni, S., & Trumbore, S. E. (2017). The muddle of ages, turnover, transit, and residence times in the carbon cycle. *Global Change Biology*, *23*(5), 1763–1773. https://doi.org/10.1111/gcb.13556

Sierra, C. A., Quetin, G. R., Metzler, H., & Müller, M. (2023). A decrease in the age of respired carbon from the terrestrial biosphere and increase in the asymmetry of its distribution. *Philosophical Transactions of the Royal Society A*, *381*(2261), 20220200. https://doi.org/10.1098/rsta.2022.0200

Solly, E. F., Brunner, I., Helmisaari, H.-S., Herzog, C., Leppälammi-Kujansuu, J., Schöning, I., et al. (2018). Unravelling the age of fine roots of temperate and boreal forests. *Nature Communications*, *9*(1), 3006. https://doi.org/10.1038/s41467-018-05460-6

Soulet, G., Skinner, L. C., Beaupré, S. R., & Galy, V. (2016). A note on reporting of reservoir ^{14}C disequilibria and age offsets. *Radiocarbon*, *58*(1), 205–211. https://doi.org/10.1017/rdc.2015.22

Steinhof, A., Altenburg, M., & Machts, H. (2017). Sample preparation at the Jena ^{14}C laboratory. *Radiocarbon*, *59*(3), 815–830. https://doi.org/10.1017/rdc.2017.50

Stroeven, A. P., Hättestrand, C., Kleman, J., Heyman, J., Fabel, D., Fredin, O., et al. (2016). Deglaciation of fennoscandia. *Quaternary Science Reviews*, *147*, 91–121. https://doi.org/10.1016/j.quascirev.2015.09.016

Stuiver, M., & Polach, H. A. (1977). Discussion reporting of ^{14}C data. *Radiocarbon*, *19*(3), 355–363. https://doi.org/10.1017/s0033822200003672

Suess, H. E. (1955). Radiocarbon concentration in modern wood. *Science*, *122*(3166), 415–417. https://doi.org/10.1126/science.122.3166.415.b

Suetsugu, K., Matsubayashi, J., & Tayasu, I. (2020). Some mycoheterotrophic orchids depend on carbon from dead wood: Novel evidence from a radiocarbon approach. *New Phytologist*, *227*(5), 1519–1529. https://doi.org/10.1111/nph.16409

Tangarife-Escobar, A., Guggenberger, G., Feng, X., Dai, G., Urbina-Malo, C., Azizi-Rad, M., & Sierra, C. A. (2024). Moisture and temperature effects on the radiocarbon signature of respired carbon dioxide to assess stability of soil carbon in the Tibetan plateau. *Biogeosciences*, *21*(5), 1277–1299. https://doi.org/10.5194/bg-21-1277-2024

Tangarife-Escobar, A., Guggenberger, G., FengX., Muñoz, E., Chanca, I., Peichl, M., et al. (2024). Radiocarbon Isotopic Disequilibrium Shows Little Incorporation of New Carbon in Mineral Soils of a Boreal Forest Ecosystem. *Zenodo*. https://doi.org/10.5281/zenodo.10952030

Tans, P. P. (1980). On calculating the transfer of carbon-13 in reservoir models of the carbon cycle. *Tellus*, *32*(5), 464–469. https://doi.org/10.3402/tellusa.v32i5.10601

Tans, P. P., Berry, J. A., & Keeling, R. F. (1993). Oceanic ^{13}C/^{12}C observations: A new window on ocean CO_2 uptake. *Global Biogeochemical Cycles*, *7*(2), 353–368. https://doi.org/10.1029/93gb00053

Thompson, M. V., & Randerson, J. T. (1999). Impulse response functions of terrestrial carbon cycle models: Method and application. *Global Change Biology*, *5*(4), 371–394. https://doi.org/10.1046/j.1365-2486.1999.00235.x

Torn, M. S., Lapenis, A. G., Timofeev, A., Fischer, M. L., Babikov, B. V., & Harden, J. W. (2002). Organic carbon and carbon isotopes in modern and 100-year-old-soil archives of the Russian steppe. *Global Change Biology*, *8*(10), 941–953. https://doi.org/10.1046/j.1365-2486.2002.00477.x

Trumbore, S. E. (2000). Age of soil organic matter and soil respiration: Radiocarbon constraints on belowground c dynamics. *Ecological Applications*, *10*(2), 399–411. https://doi.org/10.1890/1051-0761(2000)010[0399:aosoma]2.0.co;2

Trumbore, S. E., Chadwick, O. A., & Amundson, R. (1996). Rapid exchange between soil carbon and atmospheric carbon dioxide driven by temperature change. *Science*, *272*(5260), 393–396. https://doi.org/10.1126/science.272.5260.393

Trumbore, S. E., Davidson, E. A., Barbosa de Camargo, P., Nepstad, D. C., & Martinelli, L. A. (1995). Belowground cycling of carbon in forests and pastures of eastern Amazonia. *Global Biogeochemical Cycles*, *9*(4), 515–528. https://doi.org/10.1029/95gb02148

Valentini, R., Matteucci, G., Dolman, A., Schulze, E.-D., Rebmann, C., Moors, E., et al. (2000). Respiration as the main determinant of carbon balance in European forests. *Nature*, *404*(6780), 861–865. https://doi.org/10.1038/35009084

Vanguelova, E., Bonifacio, E., De Vos, B., Hoosbeek, M., Berger, T., Vesterdal, L., et al. (2016). Sources of errors and uncertainties in the assessment of forest soil carbon stocks at different scales—Review and recommendations. *Environmental Monitoring and Assessment*, *188*(11), 1–24. https://doi.org/10.1007/s10661-016-5608-5

von Fromm, S. F., Hoyt, A. M., Sierra, C. A., Georgiou, K., Doetterl, S., & Trumbore, S. E. (2024). Controls and relationships of soil organic carbon abundance and persistence vary across pedo-climatic regions. *Global Change Biology*, *30*(5), e17320. https://doi.org/10.1111/gcb.17320

Walker, J. C., Xu, X., Fahrni, S. M., Lupascu, M., & Czimczik, C. I. (2015). Developing a passive trap for diffusive atmospheric ^{14}CO_2 sampling. *Nuclear Instruments and Methods in Physics Research Section B: Beam Interactions with Materials and Atoms*, *361*, 632–637. https://doi.org/10.1016/j.nimb.2015.05.030

Wotte, A., Wordell-Dietrich, P., Wacker, L., Don, A., & Rethemeyer, J. (2017). ^{14}CO_2 processing using an improved and robust molecular sieve cartridge. *Nuclear Instruments and Methods in Physics Research Section B: Beam Interactions with Materials and Atoms*, *400*, 65–73. https://doi.org/10.1016/j.nimb.2017.04.019

Xiao, L., Wang, G., Chang, J., Chen, Y., Guo, X., Mao, X., et al. (2023). Global depth distribution of belowground net primary productivity and its drivers. *Global Ecology and Biogeography*, *32*(8), 1435–1451. https://doi.org/10.1111/geb.13705

Xiao, L., Wang, G., Wang, M., Zhang, S., Sierra, C. A., Guo, X., et al. (2022). Younger carbon dominates global soil carbon efflux. *Global Change Biology*, *28*(18), 5587–5599. https://doi.org/10.1111/gcb.16311

Xiong, X., Zhou, W., Cheng, P., Wu, S., Niu, Z., Du, H., et al. (2017). $\delta^{14}CO_2$ from dark respiration in plants and its impact on the estimation of atmospheric fossil fuel CO_2. *Journal of Environmental Radioactivity*, *169*, 79–84. https://doi.org/10.1016/j.jenvrad.2017.01.003

Yang, H., Ciais, P., Frappart, F., Li, X., Brandt, M., Fensholt, R., et al. (2023). Global increase in biomass carbon stock dominated by growth of northern young forests over past decade. *Nature Geoscience*, *16*(10), 1–7. https://doi.org/10.1038/s41561-023-01274-4

Zhao, B., Zhuang, Q., Shurpali, N., Köster, K., Berninger, F., & Pumpanen, J. (2021). North American boreal forests are a large carbon source due to wildfires from 1986 to 2016. *Scientific Reports*, *11*(1), 7723. https://doi.org/10.1038/s41598-021-87343-3